ELSEVIER

Journal of Organometallic Chemistry 627 (2001) 109–120

Journal of Organometallic Chemistry

www.elsevier.nl/locate/jorganchem

Cyclic organohydroborate complexes of metallocenes Part VI. Syntheses and structures of $Cp_2M\{(\mu\text{-}H)_2BR_2\}$ (M = Ti, Nb; $R_2 = C_4H_8$, C_5H_{10}, C_8H_{14})

Fu-Chen Liu, Christine E. Plečnik, Shengming Liu, Jianping Liu, Edward A. Meyers, Sheldon G. Shore *

Department of Chemistry, Newman & Wolfrom Laboratory, The Ohio State University, 100 West 18th Avenue, Columbus, OH 43210-1185, USA

Received 18 December 2000; accepted 12 February 2001

Abstract

The complexes, $Cp_2M\{(\mu\text{-}H)_2BC_4H_8\}$ (**1**: M = Ti; **2**: M = Nb), $Cp_2M\{(\mu\text{-}H)_2BC_5H_{10}\}$ (**3**: M = Ti; **4**: M = Nb), and $Cp_2M\{(\mu\text{-}H)_2BC_8H_{14}\}$ (**5**: M = Ti; **6**: M = Nb), were prepared from the reactions of Cp_2MCl_2 with the organohydroborate salts, $K[H_2B_2(\mu\text{-}H)(\mu\text{-}C_4H_8)_2]$, $K[H_2BC_5H_{10}]$, and $K[H_2BC_8H_{14}]$, respectively. In these reactions, the transition metal is reduced from M(IV) to M(III), producing 17-electron, paramagnetic titanocene complexes (**1**, **3** and **5**) and eighteen electron, diamagnetic niobocene complexes (**2**, **4** and **6**). Single crystal X-ray structures of **1**–**6** were determined. The molecular structure of $Cp_2Nb\{(\mu\text{-}H)_2BH_2\}$ (**7**) was redetermined using modern CCD techniques.

Keywords: Titanocene; Niobocene; Organohydroborates; Hydridoborates; Crystal structures

1. Introduction

Of the known organohydroborate metal complexes, most are derived from the lanthanide metals [1]. Several late transition metal organohydroborate complexes, which include Ni, Cu, Ag, and Ru, have also been reported [2]. While organohydroborate complexes of Zr are the only early transition metal compounds to have been studied extensively [3], several niobocene [4] and a few titanocene [5] compounds have been prepared. The Group V compounds with the formula $Cp_2M(H_2BR_2)$ are structurally interesting because the bonding interactions between the boron-containing ligand and the metal are thought to lie along the continuum of d^0 dihydride boryls (**A** of Scheme 1), d^2 hydridoborates (**B**), and d^2 hydride borane σ-complexes (**C**) [4c,e,g]. To our knowledge, the niobocene complexes include $Cp_2Nb(H_2BR_2)$ ($R_2 = H_2$ [4a,b], C_8H_{14} [4c], Cat (Cat = $O_2C_6H_4$) [4c]), $Cp^*_2Nb(H_2BR_2)$ ($R_2 = H_2$ [4d], Cat [4e], $O_2C_6H_3$-3-^{t}Bu [4e], $O_2C_6H_3$-4-^{t}Bu [4e]), and $Cp'_2Nb(H_2BR_2)$ ($Cp' = \eta^5\text{-}C_5H_4SiMe_3$; $R_2 = H_2$, C_8H_{14}, Cat) [4g]. The titanocene complexes include the Ti(III) hydridoborates, $Cp_2Ti(H_2BR_2)$ ($R_2 = H_2$ [5a,b], $(C_6F_5)_2$ [5c,d]), and the Ti(II) borane σ-compounds, $Cp_2Ti(HBCat)_a$ [5e] and its derivatives [5f,g].

Recently, several cyclic organohydroborate metallocene complexes were prepared in this laboratory. Our methodology exploits the chelating ability of the organohydroborate anions, $[H_2BR_2]^-$ ($R_2 = C_4H_8$, C_5H_{10}), as bidentate ligands. In a typical reaction, Cp_2MCl_2 (M = Zr, Hf) is reacted with the potassium salt of the organohydroborate anion to produce a metallocene double hydrogen-bridged complex (Scheme 2). A unique disproportionation of the organohydroborate anion has been observed in the reactions of $K[H_2B_2(\mu\text{-}H)(\mu\text{-}C_4H_8)_2]$ [6] with Cp_2MCl_2 to form the cyclopentaborate complexes, $Cp_2MCl\{(\mu\text{-}H)_2BC_4H_8\}$ [7]. Similarly, the cyclohexaborate derivatives, $Cp_2MCl\{(\mu\text{-}H)_2BC_5H_{10}\}$, were prepared from $K[H_2BC_5H_{10}]$ [8a]. Several derivatives of these metallocene cyclopentaborates [7,8] and cyclohexaborates [8] have been synthesized and their chemical properties studied.

In the present work, we extended syntheses of metallocene organohydroborates to titanocene and niobo-

* Corresponding author. Tel.: +1-614-2926000; fax: +1-614-2921685.

E-mail address: shore.1@osu.edu (S.G. Shore).

0022-328X/01/$ - see front matter
PII: S0022-328X(01)00727-6

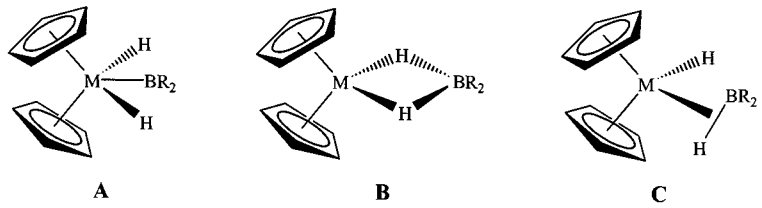

Scheme 1. Structural possibilities for Group V $Cp_2M(H_2BR_2)$ compounds. **A**, d^0 dihydride boryl; **B**, d^2 hydridoborate; and **C**, d^2 hydride borane σ-complex.

cene including the hydroborate anion, $[H_2BC_8H_{14}]^-$, of 9-borabicyclononane (9-BBN) [9]. Our interests in these compounds include expanding the relatively small library of existing early transition metal metallocene organohydroborates and understanding their reactivity and structural features. In this contribution, we report the preparation and structures of the titanocene and niobocene organohydroborates.

2. Results and discussion

*2.1. Preparation of $Cp_2M\{(\mu\text{-}H)_2BC_4H_8\}$ (**1**: M = Ti; **2**: M = Nb), $Cp_2M\{(\mu\text{-}H)_2BC_5H_{10}\}$ (**3**: M = Ti; **4**: M = Nb), and $Cp_2M\{(\mu\text{-}H)_2BC_8H_{14}\}$ (**5**: M = Ti; **6**: M = Nb)*

The metallocene organohydroborates, **1**–**6**, were prepared through reactions of a 1:2 molar ratio of Cp_2MCl_2 (M = Ti, Nb) with the potassium salt of the corresponding cyclic organohydroborate anion, $[H_2B_2(\mu\text{-}H)(\mu\text{-}C_4H_8)_2]^-$ (Eq. (1)) or $[H_2BR_2]^-$ (R_2 = C_5H_{10}, C_8H_{14}) (Eq. (2)).

In these reactions, one mole of the organohydroborate anion serves to reduce M(IV) to M(III) with the evolution of H_2, while the second mole forms the double hydrogen-bridged metallocene complex. Titanocene compounds, **1**, **3**, and **5**, are 17 electron paramagnetic complexes, while the niobocene derivatives, **2**, **4**, and **6**, are 18-electron diamagnetic complexes. The reduction of M(IV) to generate the metallocene organohydroborates parallels the reduction reactions that produce the metallocene tetrahydroborates, $Cp_2Nb\{(\mu\text{-}H)_2BH_2\}$ (**7**) [4a,b] and $Cp_2Ti\{(\mu\text{-}H)_2BH_2\}$ [5a,b]. A notable difference between Eqs. (1) and (2) is that the cyclic organohydroborate anion, $[H_2B_2(\mu\text{-}H)(\mu\text{-}C_4H_8)_2]^-$, undergoes disproportionation, which as described in Scheme 2 has also been observed in reactions of this anion with zirconocene and hafnocene dichlorides [7]. The formation of the parent organodiboranes has been verified by ^{11}B-NMR. The resonance of each organodiborane appears as a broad unresolved triplet in ether at 28.5 ppm for $B_2(\mu\text{-}H)_2(\mu\text{-}C_4H_8)_2$, 25.9 ppm for $(\mu\text{-}H)_2(BC_5H_{10})_2$, and 28.3 ppm for $(\mu\text{-}H)_2(BC_8H_{14})_2$. Complex

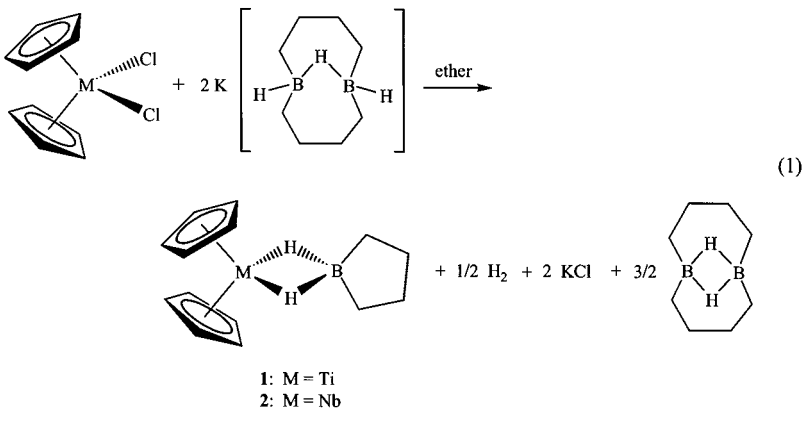

(1)

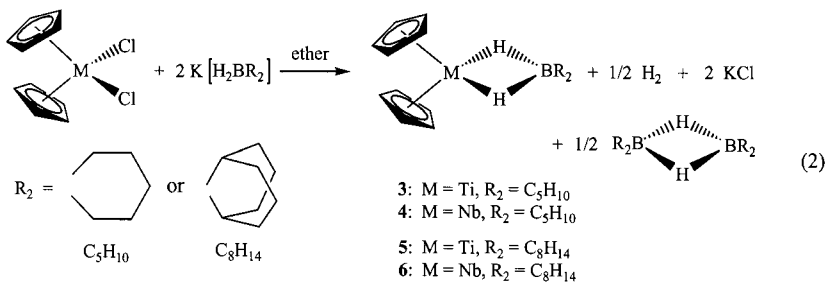

(2)

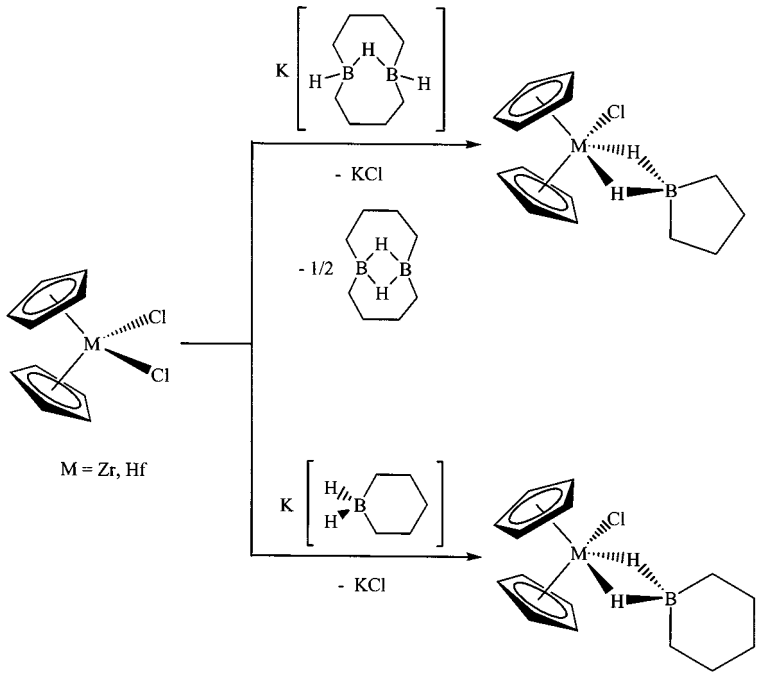

Scheme 2. Syntheses of metallocene (M = Zr, Hf) cyclic pentaborates and hexaborates.

5 has not been previously reported, but the niobocene analogue, **6**, has been prepared through the reaction of Cp_2NbH_3 with 9-BBN resulting in the loss of H_2 [4c]. Although the authors [4c] do not report a yield for **6**, the synthesis presented here appears to be more straightforward based upon a comparison of the procedures to prepare the starting materials, $K[H_2BC_8H_{14}]$ and Cp_2NbH_3. The salt, $K[H_2BC_8H_{14}]$, is prepared by a simple procedure in essentially quantitative yield [9], whereas Cp_2NbH_3 is prepared in 70–90% yields through a more involved process [10]. The only other early transition metal metallocene derivative of 9-BBN to have been reported is $Cp'_2Nb\{(\mu\text{-}H)_2BC_8H_{14}\}$ [4g].

2.2. NMR spectral studies

Proton NMR spectra of **1**, **3**, and **5** are shown in Fig. 1. As a consequence of the paramagnetism of the Ti(III) metal center, cyclopentadienide protons, bridge protons, boron nuclei, and the α-protons of the organohydroborate rings are all NMR silent. The only detectable signal in the ^{1}H-NMR spectrum of **1** is a slightly broad resonance at 1.50 ppm, assigned to the β-protons of the boracyclopentane ring. For **3**, the two resonances at 2.59 and 1.31 ppm are designated as the β- and γ-protons, respectively, of the boracyclohexane ring. These assignments are based on integration and a proton detected ^{1}H–^{13}C correlation experiment (HMQC). The sharper resonance at 1.31 ppm is consistent with the γ-protons being further away from the paramagnetic center. The sequence of the chemical shifts for the β- and γ-protons on the boracyclohexane ring in **3** follows the trend for the zirconocene complexes (from downfield to upfield the order is β, γ, then α) [8a,b]. An extremely broad resonance at around −5.1 ppm also appears in the ^{1}H-NMR spectrum of **3**, but we do not have a definitive assignment for this peak. Four broad resonances are observed in the ^{1}H-NMR spectrum of **5**. Unlike the β-protons in **1** and **3**, the β-protons (labeled as H_A and H_B in Fig. 1) in **5** are diastereotopic. The same is true for the γ-protons (H_C and H_D). Utilizing integration and a carbon detected ^{1}H–^{13}C correlation experiment (HETCOR), resonances at 3.81 and −0.08 ppm are designated as the two distinct sets of β-protons and the peaks at 2.33 and 0.60 ppm are assigned to the two sets of γ-protons. The coupling between the diastereotopic protons was not observed due to the broad line widths of the resonances. Another extremely broad resonance downfield at 10.6 ppm is also found in the ^{1}H-NMR spectrum of **5**. The typical broad line widths of the ^{1}H-NMR resonances for **1**, **3**, and **5** are caused by the paramagnetic effect rather than the quadrupole moment of the ^{11}B nucleus, since the ^{1}H spectra did not sharpen after broad band ^{11}B decoupling.

The ^{1}H-NMR spectra of **2**, **4**, and **6** are relatively straightforward. The bridging protons in these complexes are equivalent and appear as a single broad resonance upfield at −14.87 for **2**, −15.24 for **4**, and −15.21 ppm for **6**. This result is consistent with the C_{2v} symmetry of the molecular structures. Contrary to these niobocene complexes, two broad resonances are observed at about 10 ppm downfield for the inequivalent bridging protons of the zirconocene organohydro-

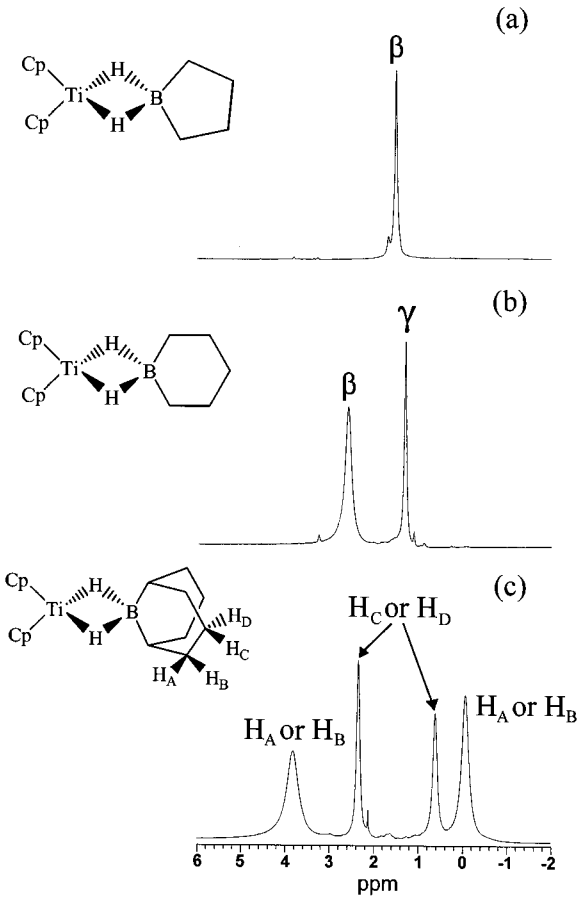

Fig. 1. ^{1}H-NMR spectra (400 MHz) of (a) $Cp_2Ti\{(\mu\text{-}H)_2BC_4H_8\}$ (**1**), (b) $Cp_2Ti\{(\mu\text{-}H)_2BC_5H_{10}\}$ (**3**), and (c) $Cp_2Ti\{(\mu\text{-}H)_2BC_8H_{14}\}$ (**5**) in C_6D_6.

Table 1
^{11}B-NMR chemical shifts (ppm) for $Cp_2Nb(H_2BR_2)$ compounds

Compound	δ [a]
$Cp_2Nb\{(\mu\text{-}H)_2BC_4H_8\}$ (**2**)	61.3
$Cp_2Nb\{(\mu\text{-}H)_2BC_5H_{10}\}$ (**4**)	55.1
$Cp_2Nb\{(\mu\text{-}H)_2BC_8H_{14}\}$ (**6**)	59.1, 59.7 [b]
Endo-$Cp_2Nb(H_2BCat)$ [c]	59
Endo-$Cp^*_2Nb\{(\mu\text{-}H)_2BCat\}$ [d]	60.2
Endo-$Cp^*_2Nb\{(\mu\text{-}H)_2BO_2C_6H_3\text{-}3\text{-}^tBu\}$ [d]	60.9
Endo-$Cp^*_2Nb\{(\mu\text{-}H)_2BO_2C_6H_3\text{-}4\text{-}^tBu\}$ [d]	60.0
$Cp'_2Nb\{(\mu\text{-}H)_2BCat\}$ [e]	54.5
$Cp'_2Nb\{(\mu\text{-}H)_2BC_8H_{14}\}$ [e]	57.6
$Cp_2Nb\{(\mu\text{-}H)_2BH_2\}$ (**7**) [d,f]	40.5
$Cp^*_2Nb\{(\mu\text{-}H)_2BH_2\}$ [d,g]	43.4
$Cp'_2Nb\{(\mu\text{-}H)_2BH_2\}$ [e]	40.0

[a] ^{11}B-NMR spectra were recorded in C_6D_6 and are externally referenced to $BF_3{\cdot}OEt_2$.
[b] Ref. [4c].
[c] Ref. [4c]; Cat = $O_2C_6H_4$.
[d] Ref. [4e].
[e] Ref. [4g]; Cp′ = η^5-$C_5H_4SiMe_3$.
[f] Ref. [4a,b].
[g] Ref. [4d].

borates [7,8]. The upfield chemical shift of the niobocene complexes may be attributed to the shielding effect of the lone pair of electrons on the Nb(III) center. The cyclopentadienyl hydrogens for **2**, **4**, and **6** appear at ca. 4.9 ppm. The proton assignments for the boracyclopentane and boracyclohexane rings in **2** and **4** are based on integration and comparison with the zirconocene analogues [7,8]. For the borabicyclononane ring the α-protons appear upfield as a broad signal at 1.29 ppm. As with **5**, the β- and γ-protons are diastereotopic. The β-proton resonances are observed as two multiplets at 1.83–1.88 and 1.54–1.68 ppm and similarly, the γ-proton resonances are located at 1.97–2.10 ppm and within the multiplet for the β-hydrogens at 1.54–1.68 ppm.

The ^{11}B-NMR spectra of **2**, **4**, and **6** consist of a broad unresolved triplet at 61.3, 55.1, and 59.1 ppm, respectively. Compared with **2**, **4**, and **6**, analogous cyclic organohydroborate zirconocene complexes have ^{11}B resonances appearing upfield in the range of 16–31 ppm [8d]. Cyclopentaborate zirconocene complexes have chemical shifts that are downfield to those of the cyclohexaborate derivatives [8d] and this trend is maintained for **2** and **4**. The ^{11}B chemical shift for **6** is the same as that reported earlier (59.7 ppm) [4c]. Table 1 lists the ^{11}B resonances for **2**, **4**, **6**, and other $Cp_2Nb(H_2BR_2)$ compounds reported in the literature. The chemical shifts of **2**, **4**, and **6** are consistent with other niobocene organohydroborates such as *endo*-$Cp^*_2Nb\{(\mu\text{-}H)_2BR_2\}$ (R_2 = Cat, $O_2C_6H_3$-3-^{t}Bu, $O_2C_6H_3$-4-^{t}Bu; around 60 ppm) [4e], $Cp'_2Nb\{(\mu\text{-}H)_2BC_8H_{14}\}$ (57.6 ppm) [4g], and $Cp'_2Nb\{(\mu\text{-}H)_2BCat\}$ [4g] (probably a hydridoborate but a boryl interaction could not be excluded; 54.5 ppm). Surprisingly, *endo*-$Cp_2Nb(H_2BCat)$, which in the solid state exists as a d^0 dihydride boryl but in solution is proposed to exist in equilibrium between the boryl and the d^2 hydridoborate, has an ^{11}B resonance (59 ppm) similar to **6** and between those of **2** and **4** [4c]. Based solely on the ^{11}B chemical shifts for **2**, **4**, **6**, and the aforementioned niobocene compounds, the boryl and hydridoborate complexes cannot be clearly distinguished from each other since they all fall within the 54–62 ppm range [4e]. As a reference, the niobocene tetrahydroborates, $Cp_2Nb\{(\mu\text{-}H)_2BH_2\}$ (**7**) (40.5 ppm) [4a,b,e], $Cp^*_2Nb\{(\mu\text{-}H)_2BH_2\}$ (43.4 ppm) [4d,e], and $Cp'_2Nb\{(\mu\text{-}H)_2BH_2\}$ (40.0 ppm) [4g], typically have ^{11}B chemical shifts farther upfield.

2.3. Molecular structures

The molecular structures of **1**–**7** were determined by single crystal X-ray diffraction analyses; structures are shown in Figs. 2–4. Crystallographic data and selected interatomic distances and bond angles can be found in Tables 2–6. The molecular structure of **6** has been

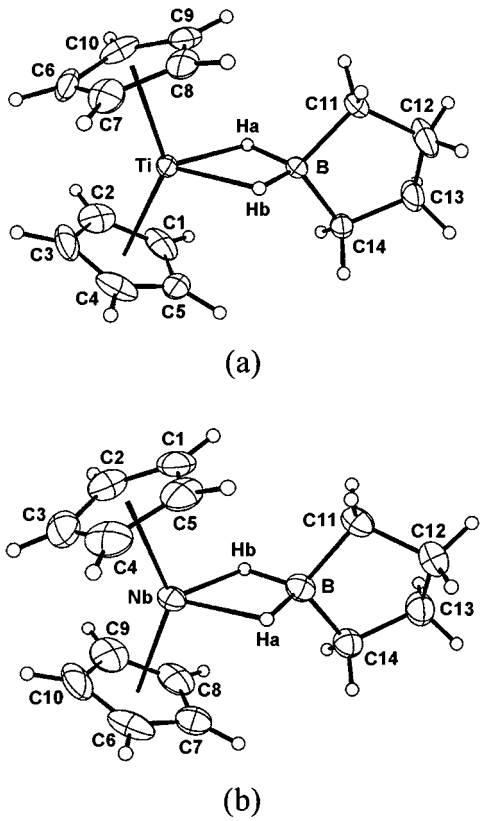

Fig. 2. Molecular structures of (a) $Cp_2Ti\{(\mu\text{-}H)_2BC_4H_8\}$ (**1**), showing 25% probability thermal ellipsoids, and (b) $Cp_2Nb\{(\mu\text{-}H)_2BC_4H_8\}$ (**2**), showing 50% probability thermal ellipsoids. Hydrogen atoms attached to carbon atoms are shown with arbitrary thermal ellipsoids for clarity.

reported by Hartwig and De Gala [4c] and since the results obtained in this laboratory are very similar to theirs, a complete list of interatomic distances and bond angles is reported only in the supplementary material.

Originally, the structure of **7** was elucidated by photographic methods at room temperature [11]. This structure successfully established the coordination of the tetrahydroborate ligand, but as noted by the authors there were several complications. The instability of the crystals, the lack of absorption correction, the rotational disorder of the cyclopentadienyl rings, the collection of the crystallographic data by photographic methods, and the relatively small number of reflections all contributed to the low accuracy in the atomic positions [11]. Futhermore, upon comparison of the structural data of **4**–**6** to the published structure of **7**, the Nb···B distance in **7** (2.26 Å) appeared unreasonably short (see Table 7). This discrepancy is not evident when **1**–**3** are compared with the structure of $Cp_2Ti\{(\mu\text{-}H)_2BH_2\}$ [12] (Table 7). In order to compare more accurately the structural features of the tetrahydroborate, **7**, to those of **1**–**6**, redetermination of the molecular structure of **7** utilizing modern CCD techniques was necessary. From the results of this laboratory, the space group was determined to be $Cmc2_1$ and not $Fmm2$ [11] as was first thought. The selection of $Fmm2$ is understandable since the hkl reflections (where $h+k$, $k+l=2n$) are relatively weak and could be considered systematically absent if intensities were detected visually.

The molecular structures of **1**–**7** are similar to each other with the coordination geometry about the metal center and boron atom best described as pseudo-tetrahedral. The centers of the two cyclopentadienyl rings and the two bridge hydrogens which connect the boron atom of the cyclic organohydroborate ring or the hydridoborate (in the case of **7**) to the metal center define the distorted tetrahedral coordination geometry of the metal. In compound **4**, a crystallographically imposed mirror plane passes through Nb, B, C(8), and the two bridging hydrogens, H(A) and H(B), to generate the second half of the molecule. In compound **7**, a crystallographically imposed mirror plane passes through Nb(1), C(13), C(16), B(1), and the two terminal hydrogens, H(2) and H(3), to generate the second half of the

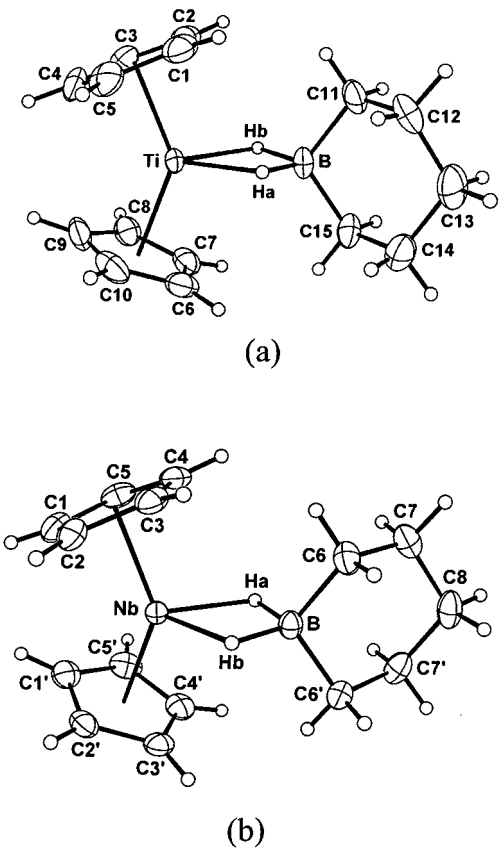

Fig. 3. Molecular structures of (a) $Cp_2Ti\{(\mu\text{-}H)_2BC_5H_{10}\}$ (**3**), showing 50% probability thermal ellipsoids, and (b) $Cp_2Nb\{(\mu\text{-}H)_2BC_5H_{10}\}$ (**4**), showing 50% probability thermal ellipsoids. For **4**, a crystallographically imposed mirror plane passes through Nb, H(A), H(B), B, and C(8) to generate the second half of the molecule. Hydrogen atoms attached to carbon atoms are shown with arbitrary thermal ellipsoids for clarity.

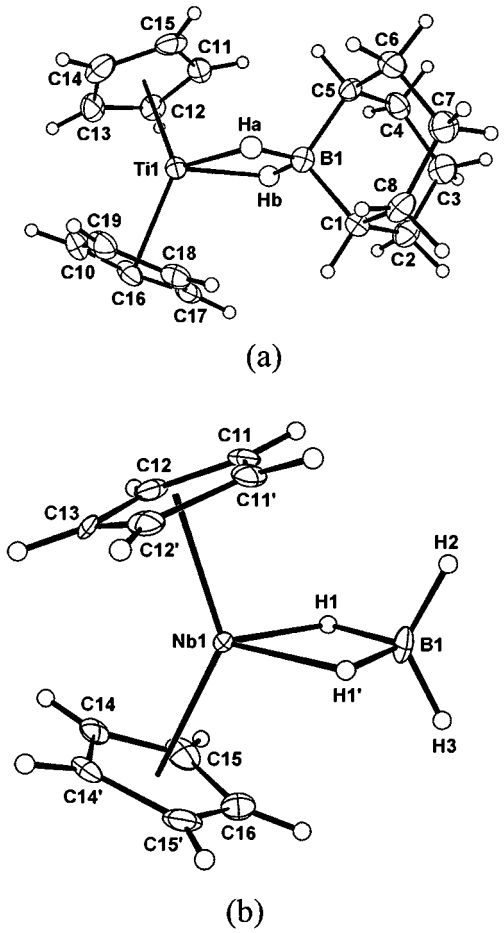

Fig. 4. Molecular structures of (a) $Cp_2Ti\{(\mu\text{-}H)_2BC_8H_{14}\}$ (**5**), showing 50% probability thermal ellipsoids, and (b) $Cp_2Nb\{(\mu\text{-}H)_2BH_2\}$ (**7**), showing 25% probability thermal ellipsoids. For **7**, a crystallographically imposed mirror plane passes through Nb(1), C(13), C(16), B(1), H(2), and H(3) to generate the second half of the molecule. Hydrogen atoms attached to carbon atoms are shown with arbitrary thermal ellipsoids for clarity.

molecule. The bridging hydrogen atoms were located and refined isotropically for all of the complexes. These hydrogens were found to be symmetrically disposed about the metal and boron atoms; that is, the two M–H_b and the two B–H_b distances for each complex are approximately equal.

Important bond distances and bond angles for **1**–**7** and other $Cp_2M(H_2BR_2)$ (M = Ti, Nb) compounds found in the literature are summarized in Table 7. In Table 7, two sets of data are listed for **6** and **7**. One set was obtained from this laboratory and the other set from Hartwig et al. [4c] for **6** and Struchkov et al. [11] for **7**. The Ti···B distances in **1** (2.409(4)), **3** (2.446(3)), and **5** (2.428(2) Å) are slightly longer than their niobocene counterparts, **2** (2.371(3)), **4** (2.427(3)), and **6** (2.411(5) Å), with the largest difference between **1** and **2**. This is surprising considering that titanium and niobium have similar covalent radii (1.43 and 1.45 Å, respectively) and that the trend is not as apparent for the metallocene tetrahydroborates, $Cp_2Ti\{(\mu\text{-}H)_2BH_2\}$ (2.37(1)) [12] and **7** (2.364(6) Å). The tetrahydroborates have somewhat shorter M– – B distances than **1**–**6**. In general, the M– – B distances for compounds **1**–**6** increase as a function of the hydroborate ligand in the following manner: cyclopentaborate < 9-borabicyclononate < cyclohexaborate. The Nb···B distances in **2**, **4**, and **6** are consistent with other d^2 Nb(III) organohydroborates such as *endo*-$Cp_2^*Nb\{(\mu\text{-}H)_2BO_2C_6H_3\text{-}3\text{-}^tBu\}$ (2.348(4) Å) [4e] and $Cp'_2Nb\{(\mu\text{-}H)_2BC_8H_{14}\}$ (2.419(5) Å) [4g]. In these types of organohydroborate complexes, the hydrogen bridges can be described as three-center two-electron bonds, with negligible 'direct' interaction between the niobium and boron atoms (See B of Scheme 1). On the other hand *endo*-$Cp_2Nb(H_2BCat)$ (2.292(5) Å), a d^0 Nb(V) hydrido-boryl in the solid state, appears to have a direct σ bond between niobium and boron [4c] (See **A** of Scheme 1). The Nb···B distance is significantly shorter than in complexes **2**, **4**, and **6**. Furthermore, this boryl complex appears to have terminal Nb–H bonds and long B–H distances suggesting little agostic interaction of boron with Nb–H. This minimal interaction between boron and hydrogen and the substantial boryl character in *endo*-$Cp_2Nb(H_2BCat)$ can be attributed to the oxygen atoms of the catechol ring which serve as π-donors to boron, thereby reducing the need for boron to accept electron density from Nb–H to form three-center bonds. Such π-donating character has been attributed to the fact that the related five-membered ring alkoxyborane, 1,3,2-dioxaborolane ($(CH_2O)_2BH$) [13a] and other oxyboron hydrides [13b] are monomers rather than hydrogen-bridged dimers. Although *endo*-$Cp_2^*Nb\{(\mu\text{-}H)_2BO_2C_6H_3\text{-}3\text{-}^tBu\}$ is a catechol derivative of *endo*-$Cp_2Nb(H_2BCat)$, the steric and electronic differences between the Cp and Cp* ligands may account for the variations in structures [4e]. Review of the structural data in Table 7 for niobocene organohydroborates and the boryl complex, *endo*-$Cp_2Nb(H_2BCat)$, reveals some features that distinguish these two types of complexes. The organohydroborates have longer Nb···B distances, longer Nb–H bonds, shorter B–H bonds, and smaller H–Nb–H and H–B–H angles than the boryl species.

3. Experimental

3.1. General procedures

All manipulations were carried out on a standard high vacuum line or in a dry box under an atmosphere of nitrogen. Diethyl ether, THF, and toluene were dried over sodium–benzophenone and freshly distilled prior to use. Hexane was stirred over concentrated sulfuric acid for two days and then decanted and washed with

Table 2
Crystallographic data for $Cp_2Ti\{(\mu\text{-}H)_2BC_4H_8\}$ (**1**), $Cp_2Ti\{(\mu\text{-}H)_2BC_5H_{10}\}$ (**3**), and $Cp_2Ti\{(\mu\text{-}H)_2BC_8H_{14}\}$ (**5**)

	1	**3**	**5**
Empirical formula	$C_{14}H_{20}BTi$	$C_{15}H_{22}BTi$	$C_{18}H_{26}BTi$
Formula weight (amu)	247.01	261.04	301.10
Temperature (°C)	−60	−60	−123
Crystal system	Monoclinic	Monoclinic	Monoclinic
Space group	$P2_1/c$	$P2_1/n$	$P2_1/n$
a (Å)	10.381(1)	11.548(1)	10.906(1)
b (Å)	8.299(1)	8.783(1)	7.904(1)
c (Å)	15.471(1)	13.872(1)	18.099(1)
β (°)	102.54(1)	103.00(1)	92.05(1)
V (Å^3)	1301.0(2)	1370.8(2)	1559.1(5)
Z	4	4	4
ρ_{calc} (g cm^{-3})	1.261	1.265	1.283
Crystal size (mm)	0.30 × 0.30 × 0.35	0.15 × 0.20 × 0.20	0.15 × 0.23 × 0.27
Radiation (λ, Å)	Mo–K_α (0.71073)	Mo–K_α (0.71073)	Mo–K_α (0.71073)
2θ limits (°)	4–50	4–50	5.62–50.04
Index ranges	$-12 \le h \le 12$, $-5 \le k \le 9$, $-18 \le l \le 18$	$-13 \le h \le 13$, $-5 \le k \le 10$, $-16 \le l \le 16$	$-12 \le h \le 12$, $-9 \le k \le 9$, $-21 \le l \le 21$
Reflections collected	4654	4927	9520
Unique reflections	2283	2417	2746
Unique reflections $[I \ge 2.0\sigma(I)]$	1663	1739	2061
Completeness to θ (%)			99.9
μ (mm^{-1})	0.627	0.599	0.536
Max/min transmission	0.9118, 0.8848	0.188, 0.114	0.9239, 0.8688
Data/restraints/parameters	2283/0/153	2417/0/162	2746/0/189
R_1 [a] $[I \ge 2.0\sigma(I)]$	0.0473	0.0590	0.0345
wR_2 [b] (all data)	0.1269	0.1133	0.0791
R_{int}	0.0364	0.1403	0.0479
Goodness-of-fit on F^2	1.039	1.061	1.013

[a] $R_1 = \Sigma||F_o| - |F_c||/\Sigma|F_o|$.
[b] $wR_2 = \{\Sigma w(F_o^2 - F_c^2)^2/\Sigma w(F_o^2)^2\}^{1/2}$.

water. Next, the hexane was dried by stirring over calcium hydride for six days, decanted and stirred over sodium–benzophenone for five days, followed by distillation into a storage bulb-containing sodium–benzophenone. Cp_2TiCl_2, Cp_2NbCl_2, and $(\mu\text{-}H)_2(BC_8H_{14})_2$ (9-BBN dimer) were purchased from Aldrich and used as received. Potassium hydride (35 wt.% dispersion in mineral oil) was purchased from Aldrich and was washed with hexane prior to use. $B_2(\mu\text{-}H)_2(\mu\text{-}C_4H_8)_2$ [14], $(\mu\text{-}H)_2(BC_5H_{10})_2$ [15], $K[H_2BC_8H_{14}]$ [9], and $Cp_2Nb\{(\mu\text{-}H)_2BH_2\}$ (**7**) [4b] were prepared by literature procedures. Elemental analyses were obtained by Galbraith Laboratories, Knoxville, TN. Proton spectra (δ (TMS) 0.00 ppm) were recorded on a Bruker AM-250 NMR spectrometer operating at 250.11 MHz and on a Bruker DPX-400 NMR spectrometer operating at 400.13 MHz. ^{11}B spectra (externally referenced to $BF_3{\cdot}OEt_2$ (δ 0.00 ppm)) were recorded at 128.38 or 80.25 MHz as noted. ^{13}C spectra were recorded on Bruker DPX-400 and DRX-500 NMR spectrometers operating at 100.6 or 125.8 MHz as noted. Infrared spectra were recorded on a Mattson Polaris Fourier Transform Spectrometer with 2 cm^{-1} resolution.

3.2. X-ray structure determination

Single crystal X-ray diffraction data were collected either on a Nonius CAD4 diffractometer using graphite monochromated Mo–K_α radiation or a Nonius KappaCCD diffraction system with graphite monochromated Mo–K_α radiation. X-ray data were obtained from single crystals of **1**–**4** on the Nonius CAD4 diffractometer. Suitable single crystals were mounted and sealed inside glass capillaries of 0.3 or 0.5 mm diameter under nitrogen. Crystallographic data were collected at −60°C. Unit cell parameters were obtained by a least-squares refinement of the angular settings from 25 reflections, well distributed in reciprocal space and lying in the 2θ range of 24–30°. The diffraction data were corrected for Lorentz and polarization effects. An empirical absorption correction was applied based on measured psi scans. X-ray data was collected from single crystals of **5**–**7** on the Nonius KappaCCD diffractometer. A single crystal was mounted on the tip of a glass fiber coated with Fomblin oil (a pentafluoro polyether). Crystallographic data was collected at −123°C. Unit cell parameters were obtained by index-

Table 3
Crystallographic data for $Cp_2Nb\{(\mu\text{-}H)_2BC_4H_8\}$ (**2**), $Cp_2Nb\{(\mu\text{-}H)_2BC_5H_{10}\}$ (**4**), $Cp_2Nb\{(\mu\text{-}H)_2BC_8H_{14}\}$ (**6**), and $Cp_2Nb\{(\mu\text{-}H)_2BH_2\}$ (**7**)

	2	**4**	**6**	**7**
Empirical formula	$C_{14}H_{20}BNb$	$C_{15}H_{22}BNb$	$C_{18}H_{26}BNb$	$C_{10}H_{14}BNb$
Formula weight (amu)	292.02	306.05	346.11	237.93
Temperature (°C)	−60	−60	−123	−123
Crystal system	Monoclinic	Orthorhombic	Monoclinic	Orthorhombic
Space group	$P2_1/n$	$Cmca$	$P2_1/c$	$Cmc2_1$
a (Å)	7.994(1)	13.770(1)	12.515(1)	9.130(1)
b (Å)	19.121(1)	8.694(1)	9.599(1)	13.522(1)
c (Å)	8.861(1)	22.827(1)	13.732(1)	7.838(1)
β (°)	110.10(1)		107.42(1)	
V (Å^3)	1271.9(2)	2732.7(3)	1574.0(2)	967.7(2)
Z	4	8	4	4
ρ_{calc} (g cm^{-3})	1.525	1.488	1.461	1.633
Crystal size (mm)	$0.22\times0.25\times0.30$	$0.12\times0.18\times0.30$	$0.08\times0.12\times0.23$	$0.15\times0.19\times0.54$
Radiation (λ, Å)	Mo–K_α (0.71073)	Mo–K_α (0.71073)	Mo–K_α (0.71073)	Mo–K_α (0.71073)
2θ limits (°)	4–50	4–60	5.26–50.10	5.38–50.04
Index ranges	$-9\le h\le9$, $-12\le k\le22$, $-10\le l\le10$	$-14\le h\le18$, $-11\le k\le10$, $-30\le l\le17$	$-14\le h\le14$, $-11\le k\le11$, $-16\le l\le16$	$-10\le h\le10$, $-15\le k\le16$, $-9\le l\le9$
Reflections collected	4549	8955	10029	2933
Unique reflections	2242	1751	2785	902
Unique reflections [$I\ge2.0\sigma(I)$]	1995	1326	2167	835
Completeness to θ (%)			99.8	100
μ (mm^{-1})	0.915	0.856	0.752	1.182
Max/min transmission	0.9317, 0.8054	0.9278, 0.7826	0.9423, 0.8460	0.8426, 0.5677
Data/restraints/parameters	2242/0/153	1751/0/89	2785/0/189	902/1/72
R_1 [$I\ge2.0\sigma(I)$]	0.0282	0.0253	0.0408	0.0206
wR_2 (all data)	0.0663	0.0517	0.1100	0.0489
R_{int}	0.0700	0.0495	0.0453	0.0268
Goodness-of-fit on F^2	1.092	1.025	1.083	1.129

ing the peaks in the first 10 frames and refined employing the whole data set. All frames were integrated and corrected for Lorentz and polarization effects using DENZO [16]. The empirical absorption correction was applied with SORTAV [17]. The structures of **1**–**7** were solved by direct methods and refined using SHELXTL (difference electron density calculations and full least-square refinements) [18]. For each structure, nonhydrogen atoms were located and refined anisotropically and the bridging hydrogen atoms and the terminal hydrogens were located and refined isotropically. All other hydrogen atoms were calculated and fixed during the refinement.

3.3. Preparation of complexes

3.3.1. $Cp_2Ti\{(\mu\text{-}H)_2BC_4H_8\}$ (**1**)

A 50 ml flask was charged with 272 mg (2.0 mmol) of $B_2(\mu\text{-}H)_2(\mu\text{-}C_4H_8)_2$, 86 mg (2.1 mmol) of KH, and 5 ml of THF. The solution was stirred at room temperature (r.t.) for 3 h. Excess KH was removed by filtration and the THF was removed under vacuum. An oily substance remained after pumping on the sample overnight. The oil became a white solid after introducing Et_2O and pumping overnight. To this flask, 249 mg (1.0 mmol) of Cp_2TiCl_2 was added. The flask was evacuated and about 15 ml of Et_2O was transferred to the system at −78°C. The system was then warmed to r.t. and stirred for 6 h. During the reaction, H_2 evolved and the solution became purple in color. The KCl was removed by filtration and the volatile materials were removed under vacuum overnight. The purple solid left in the flask was dissolved in Et_2O and kept at −40°C for crystallization. Compound **1** was isolated as purple crystals (163 mg, 66% yield). ^{1}H-NMR (C_6D_6, 400 MHz): $\delta = 1.50$ (br s, β-H). IR (KBr, cm^{-1}): 3106 (vw), 2923 (s), 2904 (s), 2865 (m), 2845 (s), 2802 (w), 2071 (vw), 1990 (vw), 1893 (m), 1852 (w), 1816 (m), 1729 (vw), 1592 (vw), 1463 (s), 1427 (br, vs), 1360 (s), 1324 (m), 1304 (m), 1264 (m), 1250 (w), 1179 (m), 1120 (w), 1055 (vw), 1017 (s), 1011 (s), 959 (vw), 907 (vw), 838 (m), 800 (br, vs), 562 (vw), 469 (vw), 434 (w). Anal. Found: C, 67.02[1]; H, 8.10. Calc. for $C_{14}H_{20}$BTi: C, 68.08; H, 8.16%.

3.3.2. $Cp_2Nb\{(\mu\text{-}H)_2BC_4H_8\}$ (**2**)

A 10 ml THF solution of the salt, $K[H_2B_2(\mu\text{-}H)(\mu\text{-}C_4H_8)_2]$ (4.05 mmol, prepared in the same manner as in

[1] The carbon analysis for **1** and for the other metallocene organohydroborates is consistently low by about 1%.

the procedure for **1**), was added dropwise to a flask containing 595 mg (2.02 mmol) of Cp_2NbCl_2 and 10 ml of THF. During this process the solution changed color to green and H_2 evolved. After stirring the system for 8 h, KCl was removed by filtration, and a green solid was left after removing THF and any low vapor-pressure species overnight. This green solid was dissolved in ether and kept at −40°C for crystallization. Compound **2** was isolated as green crystals (468 mg, 79% yield). ^{11}B-NMR (C_6D_6, 80 MHz): $\delta = 61.3$ (br t). ^{1}H-NMR (C_6D_6, 250 MHz): $\delta = 4.88$ (s, 10H, Cp), 1.73 (m, 4H, β-H), 0.81 (m, 4H, α-H), −14.87 (br s, 2H, μ-H). IR (KBr, cm^{-1}): 3115 (vw), 3106 (vw), 3090 (vw), 2936 (s), 2928 (s), 2914 (vs), 2892 (m), 2844 (s), 2806 (w), 2589 (vw), 2263 (vw), 2138 (vw), 2055 (vw), 1814 (vw), 1727 (vw), 1638 (vw), 1607 (m), 1591 (s), 1514 (vw), 1462 (vw), 1449 (vw), 1421 (m), 1353 (m), 1333 (m), 1310 (s), 1289 (s), 1248 (m), 1207 (vw), 1183 (m), 1120 (vw), 1107 (m), 1065 (w), 1034 (w), 1019 (w), 1009 (m), 995 (s), 957 (w), 926 (vw), 904 (vw), 884 (m), 847 (m), 828 (vs), 813 (m), 793 (m), 766 (vs), 725 (vw), 694 (vw), 656 (vw), 599 (vw), 563 (vw), 547 (vw), 471 (w), 403 (vw). Anal. Found: C, 56.62; H, 6.53. Calc. for $C_{14}H_{20}BNb$: C, 57.58; H, 6.90%.

Table 4
Selected interatomic distances (Å) and bond angles (°) for $Cp_2M\{(\mu\text{-}H)_2BC_4H_8\}$ (**1**: M = Ti; **2**: M = Nb)

	1	**2**
Bond distances		
Average M–C(1–5)	2.333	2.37
Average M–C(6–10)	2.343	2.37
M–Centroid$_{(C1–C5)}$	2.027	2.051
M–Centroid$_{(C6–C10)}$	2.028	2.050
M– –B	2.409(4)	2.371(3)
M–H(A)	1.84(3)	1.82(3)
M–H(B)	1.83(3)	1.76(3)
B–H(A)	1.23(3)	1.30(3)
B–H(B)	1.27(3)	1.27(3)
B–C(11)	1.615(5)	1.611(3)
B–C(14)	1.623(5)	1.619(4)
C(11)–C(12)	1.488(5)	1.534(4)
C(12)–C(13)	1.367(7)	1.525(4)
C(13)–C(14)	1.501(6)	1.534(4)
Bond angles		
Centroid–M–Centroid	139.5	140.6
Centroid$_{(C1–C5)}$–M–B	111.1	110.2
Centroid$_{(C6–C10)}$–M–B	109.4	109.2
Centroid$_{(C1–C5)}$–M–H(A)	108.5	108.2
Centroid$_{(C6–C10)}$–M–H(A)	105.1	105.7
Centroid$_{(C1–C5)}$–M–H(B)	109.6	106.6
Centroid$_{(C6–C10)}$–M–H(B)	105.9	105.7
H(A)–M–H(B)	61(1)	65(1)
H(A)–B–H(B)	97(2)	96(2)
C(11)–B–H(A)	113(1)	115(1)
C(14)–B–H(A)	114(1)	112(1)
C(11)–B–H(B)	112(2)	116(1)
C(14)–B–H(B)	118(2)	115(1)
C(11)–B–C(14)	103.9(3)	104.2(2)
B–C(11)–C(12)	104.1(3)	103.4(2)
C(11)–C(12)–C(13)	113.8(4)	104.7(2)
C(12)–C(13)–C(14)	111.7(4)	105.1(2)
B–C(14)–C(13)	104.5(3)	105.3(2)

Table 5
Selected interatomic distances (Å) and bond angles (°) for $Cp_2M\{(\mu\text{-}H)_2BC_5H_{10}\}$ (**3**: M = Ti; **4**: M = Nb [a])

	3	**4**
Bond distances		
Average M–C(1–5)	2.354	2.37
Average M–C(6–10)	2.349	
M–Centroid$_{(C1–C5)}$	2.044	2.069
M–Centroid$_{(C6–C10)}$	2.042	
M– –B	2.446(3)	2.427(3)
M–H(A)	1.88(3)	1.85(3)
M–H(B)	1.88(4)	1.85(3)
B–H(A)	1.18(3)	1.26(3)
B–H(B)	1.35(3)	1.26(3)
B–C(11)	1.603(4)	
B–C(15)	1.602(4)	
C(11)–C(12)	1.529(4)	
C(12)–C(13)	1.518(5)	
C(13)–C(14)	1.523(5)	
C(14)–C(15)	1.526(4)	
B–C(6)		1.602(3)
C(6)–C(7)		1.532(3)
C(7)–C(8)		1.523(3)
Bond angles		
Centroid–M–Centroid	141.1	142.4
Centroid$_{(C1–C5)}$–M–B	109.1	107.9
Centroid$_{(C6–C10)}$–M–B	108.3	
Centroid$_{(C1–C5)}$–M–H(A)	108.5	108.2
Centroid$_{(C6–C10)}$–M–H(A)	109.6	
Centroid$_{(C1–C5)}$–M–H(B)	101.6	102.5
Centroid$_{(C6–C10)}$–M–H(B)	103.6	
H(A)–M–H(B)	61(1)	61(1)
H(A)–B–H(B)	98(2)	97(2)
C(11)–B–H(A)	108(1)	
C(15)–B–H(A)	111(1)	
C(11)–B–H(B)	113(1)	
C(15)–B–H(B)	116(1)	
C(11)–B–C(15)	109.9(3)	
B–C(11)–C(12)	109.1(2)	
C(11)–C(12)–C(13)	112.1(3)	
C(12)–C(13)–C(14)	113.3(3)	
C(13)–C(14)–C(15)	111.7(3)	
B–C(15)–C(14)	109.7(2)	
C(6)–B–H(A)		110.9(6)
C(6)–B–H(B)		113.5(6)
C(6)–B–C(6′)		110.1(2)
B–C(6)–C(7)		110.2(2)
C(6)–C(7)–C(8)		112.4(2)
C(7)–C(8)–C(7′)		112.8(3)

[a] Symmetry transformations used to generate equivalent atoms: $-x+1, y, z$.

3.3.3. $Cp_2Ti\{(\mu\text{-}H)_2BC_5H_{10}\}$ (3)

An 82 mg (0.50 mmol) quantity of $(\mu\text{-}H)_2(BC_5H_{10})_2$, 44 mg (1.1 mmol) of KH, and about 10 ml of THF were added to a 50 ml flask. After stirring the reaction

Table 6
Selected interatomic distances (Å) and bond angles (°) for $Cp_2Ti\{(\mu\text{-}H)_2BC_8H_{14}\}$ (**5**) and $Cp_2Nb\{(\mu\text{-}H)_2BH_2\}$ (**7**) [a]

	5	7
Bond distances		
Average Ti(1)–C(11–15)	2.355	
Average Ti(1)–C(16–10)	2.356	
Ti(1)–Centroid$_{(C11–C15)}$	2.031	
Ti(1)–Centroid$_{(C16–C10)}$	2.031	
Ti(1)––B(1)	2.428(2)	
Ti(1)–H(A)	1.90(1)	
Ti(1)–H(B)	1.89(2)	
B(1)–H(A)	1.23(1)	
B(1)–H(B)	1.29(2)	
B(1)–C(1)	1.609(3)	
B(1)–C(5)	1.605(3)	
C(1)–C(2)	1.538(3)	
C(2)–C(3)	1.535(3)	
C(3)–C(4)	1.536(3)	
C(4)–C(5)	1.543(3)	
Average Nb(1)–C(11–13)		2.376
Average Nb(1)–C(14–16)		2.373
Nb(1)–Centroid$_{(C11–C13)}$		2.052
Nb(1)–Centroid$_{(C14–C16)}$		2.050
Nb(1)––B(1)		2.364(6)
Nb(1)–H(1)		1.83(4)
B(1)–H(1)		1.39(4)
B(1)–H(2)		1.22(5)
B(1)–H(3)		1.20(6)
Bond angles		
Centroid–Ti(1)–Centroid	138.5	
Centroid$_{(C11–C15)}$–Ti(1)–B(1)	110.6	
Centroid$_{(C16–C10)}$–Ti(1)–B(1)	110.8	
Centroid$_{(C11–C15)}$–Ti(1)–H(A)	109.4	
Centroid$_{(C16–C10)}$–Ti(1)–H(A)	106.2	
Centroid$_{(C11–C15)}$–Ti(1)–H(B)	105.1	
Centroid$_{(C16–C10)}$–Ti(1)–H(B)	110.2	
H(A)–Ti(1)–H(B)	61.9(6)	
H(A)–B(1)–H(B)	101(1)	
C(1)–B(1)–H(A)	114.7(7)	
C(5)–B(1)–H(A)	110.4(7)	
C(1)–B(1)–H(B)	111.2(7)	
C(5)–B(1)–H(B)	112.4(7)	
C(1)–B(1)–C(5)	107.0(2)	
B(1)–C(1)–C(2)	108.2(2)	
C(1)–C(2)–C(3)	115.6(2)	
C(2)–C(3)–C(4)	114.4(2)	
B(1)–C(5)–C(4)	108.7(2)	
C(2)–C(1)–C(8)	114.2(2)	
C(4)–C(5)–C(6)	114.5(2)	
Centroid–Nb(1)–Centroid		137.3
Centroid$_{(C11–C13)}$–Nb(1)–B(1)		108.6
Centroid$_{(C14–C16)}$–Nb(1)–B(1)		114.0
Centroid$_{(C11–C13)}$–Nb(1)–H(1)		106.0
Centroid$_{(C14–C16)}$–Nb(1)–H(1)		108.3
H(1)–Nb(1)–H(1)′		72(3)
H(1)–B(1)–H(1)′		101(3)
H(1)–B(1)–H(2)		107(2)
H(1)–B(1)–H(3)		107(2)
H(2)–B(1)–H(3)		126(6)

[a] Symmetry transformations used to generate equivalent atoms: $-x, y, z$.

mixture at r.t. for 3 h, the unreacted KH was removed by filtration, and a white solid remained when the THF was removed. Cp_2TiCl_2 (124 mg, 0.498 mmol) was then added to the flask and about 20 ml of Et_2O was condensed at −78°C. The system was warmed to r.t. and stirred for 3 h, during which time the red Cp_2TiCl_2 disappeared gradually, accompanied by evolution of H_2. The solution became purple in color and KCl formed. After filtration, Et_2O was removed and the resulting purple solid was dried under vacuum overnight. Compound **3** was isolated as purple crystals (105 mg, 80% yield) from Et_2O solution at −40°C by slow evaporation. Alternatively, crystals can be obtained from toluene at r.t. by slow evaporation of the solvent followed by washing them with cold hexane (2 × 10 ml). ^{1}H-NMR (C_6D_6, 400 MHz): $\delta = 2.59$ (br s, 4H, β-H), 1.31 (br s, 2H, γ-H), −5.1 (br s). ^{13}C-NMR (C_6D_6, 101 MHz): $\delta = 35.3$ (s, γ-C), 5.5 (br s, β-C). IR (KBr, cm^{-1}): 3108 (vw), 3090 (vw), 2921 (s), 2903 (s), 2873 (s), 2832 (m), 2812 (m), 1953 (vw), 1927 (vw), 1878 (m), 1851 (w), 1827 (m), 1777 (w), 1747 (w), 1728 (w), 1713 (w), 1460 (w), 1454 (m), 1446 (m), 1441 (m), 1425 (s), 1402 (br, vs), 1364 (m), 1336 (m), 1290 (m), 1274 (m), 1213 (m), 1128 (vw), 1123 (vw), 1097 (vw), 1089 (w), 1069 (w), 1015 (s), 954 (m), 920 (vw), 899 (vw), 846 (w), 827 (m), 809 (s), 795 (vs), 645 (br, vw), 586 (br, vw), 438 (vw). Anal. Found: C, 68.02; H, 8.37. Calc. for $C_{15}H_{22}BTi$: C, 69.02; H, 8.50%.

3.3.4. $Cp_2Nb\{(\mu\text{-}H)_2BC_5H_{10}\}$ (4)

Cp_2NbCl_2 (152 mg, 0.517 mmol) was added to a 50 ml flask containing 1.03 mmol of $K[H_2BC_5H_{10}]$ (prepared in the same manner as in the procedure for **3**). The flask was evacuated and about 5 ml of Et_2O was condensed at −78°C. The system was warmed to r.t. and the solution stirred overnight, during which time H_2 evolved. After filtration, Et_2O was removed and the resulting solid was dried under vacuum overnight. Compound **4** was isolated as green crystals (90 mg, 57% yield) from Et_2O solution at −40°C by slow evaporation. ^{11}B-NMR (C_6D_6, 80 MHz): $\delta = 55.1$ (br t). ^{1}H-NMR (C_6D_6, 250 MHz): $\delta = 4.88$ (s, 10H, Cp), 1.63 (m, 6H, β- and γ-H), 0.90 (m, 4H, α-H), −15.24 (br s, 2H, μ-H). IR (KBr, cm^{-1}): 3115 (w), 3106 (vw), 2948 (m), 2933 (m), 2909 (s), 2876 (s), 2836 (s), 2814 (m), 1592 (m), 1573 (m), 1536 (w), 1519 (w), 1454 (vw), 1423 (m), 1364 (s), 1358 (s), 1320 (vs), 1281 (w), 1258 (vw), 1222 (m), 1202 (m), 1136 (vw), 1107 (w), 1096 (vw), 1089 (vw), 1074 (w), 1070 (w), 1036 (vw), 1021 (w), 1011 (s), 998 (s), 954 (m), 920 (vw), 912 (vw), 887 (w), 850 (m), 841 (w), 830 (s), 813 (w), 794 (m), 767 (m), 617 (vw), 609 (vw), 596 (w). Anal. Found: C, 58.03; H, 7.30. Calc. for $C_{15}H_{22}BNb$: C, 58.87; H, 7.25%.

Table 7
Important interatomic distances (Å) and bond angles (°) for $Cp_2M(H_2BR_2)$ (M = Ti, Nb) compounds

Compound	M···B	M–H	B–H	H–M–H	H–B–H
$Cp_2Ti\{(\mu\text{-}H)_2BC_4H_8\}$ (**1**)	2.409(4)	1.84(3), 1.83(3)	1.23(3), 1.27(3)	61(1)	97(2)
$Cp_2Ti\{(\mu\text{-}H)_2BC_5H_{10}\}$ (**3**)	2.446(3)	1.88(3), 1.88(4)	1.18(3), 1.35(3)	61(1)	98(2)
$Cp_2Ti\{(\mu\text{-}H)_2BC_8H_{14}\}$ (**5**)	2.428(2)	1.90(1), 1.89(2)	1.23(1), 1.29(2)	61.9(6)	101(1)
$Cp_2Nb\{(\mu\text{-}H)_2BC_4H_8\}$ (**2**)	2.371(3)	1.82(3), 1.76(3)	1.30(3), 1.27(3)	65(1)	96(2)
$Cp_2Nb\{(\mu\text{-}H)_2BC_5H_{10}\}$ (**4**)	2.427(3)	1.85(3), 1.85(3)	1.26(3), 1.26(3)	61(1)	97(2)
$Cp_2Nb\{(\mu\text{-}H)_2BC_8H_{14}\}$ (**6**)	2.411(5) [a]	1.87(4), 1.89(4)	1.32(3), 1.26(5)	64(2)	101(3)
	2.40(1) [b]	1.84(6), 1.80(7)	1.38(7), 1.39(7)	70(3)	98 [c]
$Cp_2Ti\{(\mu\text{-}H)_2BH_2\}$ [d]	2.37(1)	1.75(8), 1.75(8)	1.23(8), 1.23(8)	60(5)	91(7)
$Cp_2Ti\{(\mu\text{-}H)_2B(C_6F_5)_2\}$ [e]	2.450(10) [f]	2.03, 1.97 [g]	1.32, 1.32	65.1	109.5
	2.440(3) [h]	1.91(1), 1.91(1)	1.21(1), 1.21(1)	58.2(4)	100.8(7)
$Cp_2Nb\{(\mu\text{-}H)_2BH_2\}$ (**7**)	2.364(6) [i]	1.83(4), 1.83(4)	1.39(4), 1.39(4)	72(3)	101(3)
	2.26(6) [j]	2.0(1), 2.0(1)	1.1(2), 1.1(2)	56 [c]	122(10)
$Cp^*_2Nb\{(\mu\text{-}H)_2BH_2\}$ [k]	2.35(1)	1.88(7), 1.79(8)	1.17(7), 1.16(8)	58(3)	100(5)
Endo-$Cp_2Nb(H_2BCat)$ [l]	2.292(5)	1.62(4), 1.58(5)	1.69(4), 1.62(5)	92(2)	138(2)
Endo-$Cp^*_2Nb\{(\mu\text{-}H)_2BO_2C_6H_3\text{-}3\text{-}^tBu\}$ [k]	2.348(4)	1.86(4), 1.63(4)	1.36(4), 1.46(4)	73(2)	95(2)
$Cp'_2Nb\{(\mu\text{-}H)_2BC_8H_{14}\}$ [m]	2.419(5)	1.82(4), 1.85(3)	1.38(4), 1.28(3)	66.0(15)	97(2)

[a] Results obtained in this laboratory.
[b] Ref. [4c].
[c] No estimated standard deviations were reported.
[d] Ref. [12].
[e] Two references report the molecular structure of this compound. There are two unique and independent molecules in the asymmetric unit cell. Since the structural data are similar for both of these references, we chose to list the data for only one molecule in the unit cell.
[f] Ref. [5c].
[g] Since the bridging hydrogen atoms were not refined no estimated standard deviations were calculated.
[h] Ref. [5d].
[i] Results obtained in this laboratory. The space group was determined to be $Cmc2_1$ from modern CCD techniques.
[j] Ref. [11]. The space group was determined to be *Fmm*2 by photographic methods at room temperature. Although the molecular structure establishes the coordination of the tetrahydroborate ligand, care should be taken when comparing the bond distances and angles to the above complexes due to the low accuracy in the atomic positions.
[k] Ref. [4e].
[l] Ref. [4c]; Cat = $O_2C_6H_4$.
[m] Ref. [4g]; Cp′ = η^5-$C_5H_4SiMe_3$.

3.3.5. $Cp_2Ti\{(\mu\text{-}H)_2BC_8H_{14}\}$ (5)

A 50 ml flask was charged with 421 mg (1.73 mmol) of $(\mu\text{-}H)_2(BC_8H_{14})_2$ and 156 mg (3.89 mmol) of KH. The flask was evacuated and ca. 30 ml of THF was condensed at −78°C. The flask was warmed to r.t. and stirred for 3 h. After filtering the excess KH, the solvent was removed, leaving a white solid. Cp_2TiCl_2 (427 mg, 1.71 mmol) was added to the flask and 30 ml of Et_2O was condensed at −78°C. The flask was warmed to r.t. and stirred for 3 h. The solution turned purple with evolution of H_2 and precipitation of KCl. The KCl was filtered and the volatile materials were removed. The purple solid was washed with cold hexane (3 × 15 ml). Crystals were obtained by dissolving the solid in toluene and slowly evaporating the solvent at r.t. The crystals were washed with hexane (6 × 1 ml) at r.t. and dried under vacuum. Compound **5** was isolated as purple crystals (295 mg, 57% yield). ^{1}H-NMR (C_6D_6, 400 MHz): δ = 10.6 (br s), 3.81 (br s, 4H, β-H), 2.33 (br s, 2H, γ-H), 0.60 (br s, 2H, β-H), −0.08 (br s, 4H, β-H). ^{13}C-NMR (C_6D_6, 101 MHz): δ = 28.4 (s, γ-C), 22.4 (br s, β-C). IR (KBr, cm^{-1}): 3115 (w), 3089 (w), 2971 (w), 2920 (m), 2873 (s), 2823 (s), 1889 (w), 1858 (m), 1838 (m), 1803 (m), 1762 (w), 1733 (m), 1700 (w), 1695(w), 1482 (w), 1416 (s), 1345 (m), 1282 (w), 1208 (w), 1114 (w), 1069 (w), 1059 (w), 1042 (w), 1019 (s), 923 (m), 899 (w), 808 (s), 794 (s), 746 (w). Anal. Found: C, 70.53; H, 8.70. Calc. for $C_{18}H_{26}BTi$: C, 71.80; H, 8.70%.

3.3.6. $Cp_2Nb\{(\mu\text{-}H)_2BC_8H_{14}\}$ (6)

In the dry box, 241 mg (0.82 mmol) of Cp_2NbCl_2 was added to a flask containing 1.64 mmol of $K[H_2BC_8H_{14}]$ (prepared in the same manner as in the procedure for **5**). The flask was evacuated and about 15 ml of Et_2O was condensed into the flask at −78°C. The system was warmed to r.t. and stirred overnight during which time H_2 evolved. After filtration, Et_2O was removed and the resulting solid was dried under vacuum and washed with cold hexane (3 × 2 ml). Green crystals (171 mg, 60% yield) of **6** were isolated from Et_2O solution at −40°C by slow evaporation. ^{11}B-NMR (C_6D_6, 128 MHz): δ = 59.1 (br t). ^{1}H-NMR (C_6D_6, 400 MHz): δ = 4.92 (s, 10H, Cp), 1.97–2.10 (m, 2H, γ-H), 1.83–1.88 (m, 4H, β-H), 1.54–1.68 (m, 6H, β- and γ-H), 1.29 (br s, 2H, α-H), −15.21 (br s, 2H, μ-H). IR (KBr,

cm^{-1}): 3117 (w), 3106 (w), 3096 (w), 3085 (w), 2978 (w), 2943 (m), 2916 (m), 2898 (s), 2889 (s), 2868 (s), 2826 (s), 2656 (w), 1597 (m), 1570 (m), 1450 (m), 1424 (m), 1388 (s), 1364 (s), 1317 (vs), 1307 (vs), 1284 (s), 1243 (s), 1205 (m), 1109 (m), 1070 (m), 1040 (m), 1016 (m), 997 (m), 925 (m), 891 (w), 849 (m), 824 (vs), 769 (s), 745 (m), 597 (m).

4. Supplementary material

Crystallographic data for the structural analysis (excluding structure factors) have been deposited with the Cambridge Crystallographic Data Center, CCDC Nos. 151633 (compound **1**), 151634 (compound **2**), 151635 (compound **3**), 151636 (compound **4**), 151637 (compound **5**), 154155 (compound **6**), and 154156 (compound **7**). Copies of this information may be obtained free of charge from The Director, CCDC, 12 Union Road, Cambridge CB2 1EZ, UK (fax: +44-1223-336033; e-mail: deposit@ccdc.cam.ac.uk or www: http://www.ccdc.cam.ac.uk).

Acknowledgements

This work was supported by the National Science Foundation through Grants CHE 97-00394 and CHE 99-01115. We thank Dr Karl Vermillion and Roman Kultyshev for assistance with the $^{1}H-^{13}C$ correlation experiments.

References

[1] (a) R. Shinomoto, E. Gamp, N.M. Edelstein, D.H. Templeton, A. Zalkin, Inorg. Chem. 22 (1983) 2351. (b) R. Shinomoto, A. Zalkin, N.M. Edelstein, Inorg. Chim. Acta 139 (1987) 97. (c) J. Brennan, R. Shinomoto, A. Zalkin, N.M. Edelstein, Inorg. Chem. 23 (1984) 4143. (d) R. Shinomoto, A. Zalkin, N.M. Edelstein, D. Zhang, Inorg. Chem. 26 (1987) 2868. (e) R. Shinomoto, J.G. Brennan, N.M. Edelstein, A. Zalkin, Inorg. Chem. 24 (1985) 2896. (f) P. Zanella, F. Ossola, M. Porchia, G. Rossetto, A.C. Villa, C. Guastini, J. Organomet. Chem. 323 (1987) 295. (g) T.J. Marks, J.R. Kolb, J. Am. Chem. Soc. 97 (1975) 27. (h) H.I. Schlesinger, H.C. Brown, L. Horvitz, A.C. Bond, L.D. Tuck, A.C. Walker, J. Am. Chem. Soc. 75 (1953) 222.

[2] (a) D.G. Holah, A.N. Hughes, N.I. Khan, Can. J. Chem. 62 (1984) 1016. (b) B.G. Segal, S.J. Lippard, Inorg. Chem. 16 (1977) 1623. (c) K.M. Melmed, T.-I. Li, J.J. Mayerle, S.J. Lippard, J. Am. Chem. Soc. 96 (1974) 69. (d) J.C. Bommer, K.W. Morse, Inorg. Chem. 22 (1983) 592. (e) J.C. Bommer, K.W. Morse, Inorg. Chem. 18 (1979) 531. (f) J.C. Bommer, K.W. Morse, Inorg. Chem. 19 (1980) 587. (g) R.T. Baker, J.C. Calabrese, S.A. Westcott, T.B. Marder, J. Am. Chem. Soc. 117 (1995) 8777. (h) For an example of a late transition metal dihydride boryl see: R.T. Baker, D.W. Ovenall, J.C. Calabrese, S.A. Westcott, N.J. Taylor, I.D. Williams, T.B. Marder, J. Am. Chem. Soc. 112 (1990) 9399.

[3] (a) W.K. Kot, N.M. Edelstein, A. Zalkin, Inorg. Chem. 26 (1987) 1339. (b) P. Paetzold, L. Geret, R. Boese, J. Organomet. Chem. 385 (1990) 1. (c) Y. Sun, W.E. Piers, S.J. Rettig, Organometallics 15 (1996) 4110. (d) R.E.v.H. Spence, D.J. Parks, W.E. Piers, M.-A. MacDonald, M.J. Zaworotko, S.J. Rettig, Angew. Chem. Int. Ed. Engl. 34 (1995) 1230. (e) Y. Sun, R.E.v.H. Spence, W.E. Piers, M. Parvez, G.P.A. Yap, J. Am. Chem. Soc. 119 (1997) 5132. (f) G. Erker, R. Noe, D. Wingbermühle, J.L. Petersen, Angew. Chem. Int. Ed. Engl. 32 (1993) 1213. (g) R.E.v.H. Spence, W.E. Piers, Y. Sun, M. Parvez, L.R. MacGillivray, M.J. Zaworotko, Organometallics 17 (1998) 2459.

[4] (a) C.R. Lucas, M.L.H. Green, J. Chem. Soc. Chem. Commun. (1972) 1005. (b) C.R. Lucas, Inorg. Synth. 16 (1976) 109. (c) J.F. Hartwig, S.R. De Gala, J. Am. Chem. Soc. 116 (1994) 3661. (d) R.A. Bell, S.A. Cohen, N.M. Doherty, R.S. Threlkel, J.E. Bercaw, Organometallics, 5 (1986) 972. (e) D.R. Lantero, D.L. Ward, M.R. Smith III, J. Am. Chem. Soc. 119 (1997) 9699. (f) D.R. Lantero, S.L. Miller, J.-Y. Cho, D.L. Ward, M.R. Smith III, Organometallics 18 (1999) 235. (g) A. Antiñolo, F. Carrillo-Hermosilla, J. Fernández-Baeza, S. García-Yuste, A. Otero, A.M. Rodríguez, J. Sánchez-Prada, E. Villaseñor, R. Gelabert, M. Moreno, J.M. Lluch, A. Lledós, Organometallics 19 (2000) 3654.

[5] (a) H. Nöth, R. Hartwimmer, Chem. Ber. 93 (1960) 2238. (b) C.R. Lucas, Inorg. Synth. 17 (1977) 91. (c) P.A. Chase, W.E. Piers, M. Parvez, Organometallics 19 (2000) 2040. (d) R.E. Douthwaite, Polyhedron 19 (2000) 1579. (e) J.F. Hartwig, C.N. Muhoro, X. He, O. Eisenstein, R. Bosque, F. Maseras, J. Am. Chem. Soc. 118 (1996) 10936. (f) C.N. Muhoro, X. He, J.F. Hartwig, J. Am. Chem. Soc. 121 (1999) 5033. (g) C.N. Muhoro, J.F. Hartwig, Angew. Chem. Int. Ed. Eng. 36 (1997) 1510. (h) X. He, J.F. Hartwig, J. Am. Chem. Soc. 118 (1996) 1696. (i) J.F. Hartwig, C.N. Muhoro, Organometallics 19 (2000) 30.

[6] (a) W.R. Clayton, D.J. Saturnino, P.W.R. Corfield, S.G. Shore, J. Chem. Soc. Chem. Commun. (1973) 377. (b) D.J. Saturnino, M. Yamauchi, W.R. Clayton, R.W. Nelson, S.G. Shore, J. Am. Chem. Soc. 97 (1975) 6063.

[7] (a) G.T. Jordan IV, F.-C. Liu, S.G. Shore, Inorg. Chem. 36 (1997) 5597. (b) G.T. Jordan IV, S.G. Shore, Inorg. Chem. 35 (1996) 1087.

[8] (a) J. Liu, E.A. Meyers, S.G. Shore, Inorg. Chem. 37 (1998) 496. (b) F.-C. Liu, J. Liu, E.A. Meyers, S.G. Shore, Inorg. Chem. 37 (1998) 3293. (c) F.-C. Liu, J. Liu, E.A. Meyers, S.G. Shore, Inorg. Chem. 38 (1999) 2169. (d) F.-C. Liu, B. Du, J. Liu, E.A. Meyers, S.G. Shore, Inorg. Chem. 38 (1999) 3228.

[9] R. Köster, G. Seidel, Inorg. Synth. 22 (1983) 198.

[10] J.A. Labinger, Adv. Chem. Ser. 167 (1978) 149.

[11] N.I. Kirillova, A.I. Gusev, Y.T. Struchkov, J. Struct. Chem. 15 (1974) 622.

[12] K.M. Melmed, D. Coucouvanis, S.J. Lippard, Inorg. Chem. 12 (1973) 232.

[13] (a) S.H. Rose, S.G. Shore, Inorg. Chem. 1 (1962) 744. (b) G.E. McAchran, S.G. Shore, Inorg. Chem. 5 (1966) 2044.

[14] (a) D.E. Young, S.G. Shore, J. Am. Chem. Soc. 91 (1969) 3497. (b) E. Breuer, H.C. Brown, J. Am. Chem. Soc. 91 (1969) 4164.

[15] H.C. Brown, E. Negishi, J. Organomet. Chem. 26 (1971) C67.

[16] Z. Otwinowsky, W. Minor, Processing of X-ray Diffraction Data Collected in Oscillation Mode, in: C.W. Carter Jr., R.R. Sweet (Eds.), Methods in Enzymology, vol. 276, Macromolecular Crystallography Part A, Academic Press, New York, 1997, pp. 307–326.

[17] R.H. Blessing, Acta Crystallogr. Sect. A 51 (1995) 33.

[18] SHELXTL (version 5.10), Bruker Analytical X-ray Systems, 1997.